

Theoretical Study on Polyimide–Cu(100)/Ni(100) Adhesion

Jia Zhang,^{†,‡} Michael B. Sullivan,[†] Jian Wei Zheng,[†] Kian Ping Loh,[‡] and Ping Wu^{*,†}

Institute of High Performance Computing, 1 Science Park Road, #01-01 The Capricorn, Singapore 117528, and Department of Chemistry, National University of Singapore, 3 Science Drive 3, Singapore 117543

Received December 28, 2005. Revised Manuscript Received August 31, 2006

The interfacial properties of polyimide (PI)/M(100) (M = Cu and Ni) were investigated using density functional theory (DFT). A PMDA-ODA monomer unit was used to represent the full PI and the surface was represented by periodically repeated slabs. PI prefers the bridge and top sites on a Cu(100) surface but only forms weak C=O–Cu interactions. PI favors the bridge site on a Ni(100) surface and can form strong C–Ni, N–Ni, and C=O–Ni bonds. The adsorption energies of PI on Cu(100) and Ni(100) surfaces are –0.58 and –4.7 eV, respectively. Compared to the adsorption energies of O and O₂ on a Cu(100) surface, the adsorption of PI on Cu(100) is not energetically favorable, which leads to the easy oxidation of Cu particles in a Cu/PI nanocomposite. The good adhesion at PI/Ni(100) suggests that Ni is a better candidate as a metal filler compared to Cu in the metal–polyimide composite.

1. Introduction

In recent years, polymer–metal composites have received increased attention due to the advantages of coupling of the two components.¹ Polyimides (PI) are a very useful class of polymer in microelectronic applications because of their unique properties including thermal and chemical stability, high electrical resistivity, low dielectric constant, and good processibility.^{2,3} Metals are conductors and introducing them into a polyimide matrix can in principle result in high dielectric constant composite. At present, polymers filled with high dielectric ceramics have been studied for use in thick film capacitors.^{4–6} However, the corresponding studies in metal–polymer composites are still in their infancy, which is probably related to the stability of metal particles and the reactivity to the polymer.

Zhu and Xu observed that the color of Cu/PI nanocomposite changed from red brown to green when the composite was exposed to air for a week, indicating that oxidation of Cu particles has occurred.⁷ However, no color change was observed when the composite was kept in a nitrogen atmosphere. Their findings motivated us to study Cu/PI and Ni/PI interfaces theoretically, aimed at finding the oxidation mechanism of copper particles and looking for a replacement of the copper particles for making a nanometal/PI composite.

Although the problem of adhesion between metal and polyimide remains an open issue, chemical interactions were reported to play an important role in this.^{2,8} Furthermore, embedding metal particles in a polymer matrix is the easiest and most convenient way to stabilize nanometals. Good adhesion between the metal and the PI ensures that the PI encapsulates metal particles very well, which prevents metal particles from exposure to air and hence prevents the oxidation of metal particles. Therefore, investigating interfacial interactions is very important for understanding the adhesion behavior and stability of metal in metal-filled polyimide.

In the past decade, many experimental investigations on metal/polymer interface have been reported.^{8–13} Ramos has published some papers studying the adhesion of metals to polyimide using semiempirical molecular dynamics on representative metal clusters. While there have been some semiempirical calculations,^{14–16} no detailed theoretical studies on the interfacial properties of the PI/metal interface using density functional theory (DFT) have been reported until now. In this work, we study the chemical interaction, charge transfer, and adhesion characteristics of PI/Cu(100) and PI/Ni(100) interfaces using DFT calculations.

* To whom correspondence should be addressed. E-mail: wuping@ihpc.a-star.edu.sg. Tel.: +65 6419 1212. Fax: +65 6419 1290.

[†] Institute of High Performance Computing.

[‡] National University of Singapore.

- (1) Luigi, N.; Gianfranco, C. *Metal-polymer nanocomposites*; Wiley-Interscience: Hoboken, NJ, 2005.
- (2) Ghosh, M. K.; Mittal, K. L. *Polyimides: fundamentals and applications*; Marcel Dekker: New York, 1996.
- (3) Maier, G. *Prog. Polym. Sci.* **2001**, *26*, 3–65.
- (4) Bai, Y.; Cheng, Z. Y.; Bharti, V.; Xu, H. S.; Zhang, Q. M. *Appl. Phys. Lett.* **2000**, *76*, 3804–3806.
- (5) Das-Gupta, D. K.; Doughty, K. *Thin Solid Films* **1988**, *158*, 93–105.
- (6) Xie, S.-H.; Zhu, B.-K.; Xu, Z.-K.; Xu, Y.-Y. *Mater. Lett.* **2005**, *59*, 2403–2407.
- (7) Zhu, B. K.; Xu, Z. K. Personal communication.

- (8) Kim, K. J.; Kim, K. S.; Lee, N.-E.; Choi, J.; Jung, D. *J. Vac. Sci. Technol. A* **2001**, *19*, 1072–1077.
- (9) Chiang, P.-C.; Whang, W.-T.; Tsai, M.-H.; Wu, S.-C. *Thin Solid Films* **2004**, *447–448*, 359–364.
- (10) Du, M.; Opila, R. L.; Case, C. *J. Vac. Sci. Technol. A* **1998**, *16*, 155–162.
- (11) Lee, W.-J.; Lee, Y.-S.; Rha, S.-K.; Lee, Y.-J.; Lim, K.-Y.; Chung, Y.-D.; Whang, C.-N. *Appl. Surf. Sci.* **2003**, *205*, 128–136.
- (12) Oultache, A. K.; Prud'homme, R. E. *Polym. Adv. Technol.* **2000**, *11*, 316–323.
- (13) Yang, C.-Y.; Chen, J. S.; Hsu, S. L. *C. J. Vac. Sci. Technol. A* **2005**, *23*, 862–868.
- (14) Ramos, M. M. D. *Vacuum* **2002**, *64*, 255–260.
- (15) Ramos, M. M. D.; Almeida, J. P. P. *J. Mater. Process. Technol.* **1999**, *93*, 147–150.
- (16) Ramos, M. M. D.; Stoneham, A. M.; Sutton, A. P. *Acta Metall. Mater.* **1993**, *41*, 2105–2111.

In this work, a PMDA–ODA monomer is selected as a typical polyimide. While the selection of a monomer is not ideal, it should be representative of the full system. As in all simulations, there are some simplifications required to handle complex systems. There are two ways in which to fix this problem. One would be to increase the size of the supercell. We cannot do this as our system is already nearly 20 Å long. The other way would be to create a supercell that repeated across the monomer unit. However, it is too difficult to get both the metal and polymer to “break” at the same point. This methodology is standard within the field and other results have been published.^{17,18}

Another point related to this is that because we are interested in understanding nanoparticles, a monomer should be quite representative of the system. The monomer can adhere to the metal surface of one nanometal and the next nanometal will then try to orient itself with the polyimide in such a way that there is an optimum amount of space in between. This means that the polymer can adhere in a way that is most favored, making the fact that we are dealing with a monomer less important.

We chose to study the (100) surfaces due to their simplicity and implications in some nanometals. (100) faces are found on icosahedral nanometals and should be representative of the metal–polymer interactions. While we expect the nanometals to be polymorphous and have many different faces available for bonding to polyimide, previous studies have shown that benzene adsorbs the strongest to the (100) surface compared to the (111) and (110) surfaces.¹⁹

By investigating the interfacial information and stability, we hope to learn how to control the oxidation of the nanometal and create new materials with high dielectric constant and processibility. In this work, a PMDA–ODA monomer is selected as a typical polyimide.

2. Theoretical Methods

In our calculations, density functional theory (DFT) was performed using VASP program code,^{20,21} in which a plane-wave basis set is used. The electron–ion interaction is modeled by the projector-augmented wave (PAW) method.^{22,23} The Perdew–Wang form of generalized gradient approximation (GGA) was used for the exchange and correlation function.²⁴ The plane-wave cutoff energy was set to 400 eV. The calculated lattice constant is 3.636 Å for Cu bulk and 3.512 Å for Ni bulk, in good agreement with the experimental value of 3.62 Å²⁵ and 3.524 Å,²⁶ respectively.

Cu(100) and Ni(100) surfaces are simulated by a slab supercell approach with periodic boundaries. The surface is made up of four layers of metal atoms of which the bottom two layers are frozen. We used a vacuum region corresponding to five metal layers, which is large enough to avoid interactions between slabs. For the 9 × 4

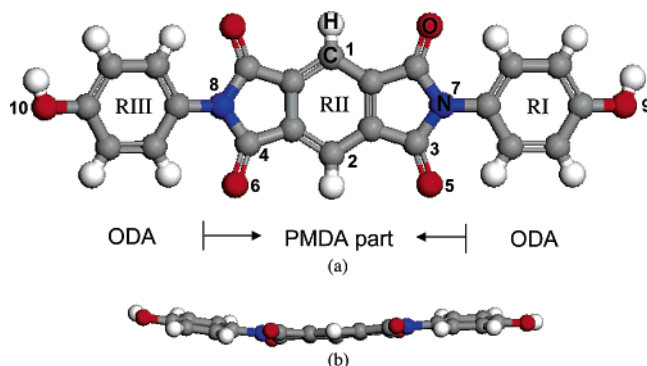


Figure 1. (a) Schematic drawing of polyimide (PMDA–ODA fragment) used in the calculation; (b) side view of optimized PMDA–ODA fragment.

Cu and Ni surfaces used in the calculations, there are 36 atoms in each layer for a total of 144 metal atoms and $1 \times 2 \times 2$ k-point mesh was used. The vacuum size, cutoff energy, and k-point mesh were tested for convergence. No symmetry conditions were imposed and the PI and top two metal layers were allowed to move freely. All these settings have been tested and surface energies were converged to better than 5 meV/atom. In addition, we tested the inclusion of spin polarization for the nickel system and found no significant change in the results, which is in agreement with previous work.¹⁹

3. Results and Discussion

3.1. Adsorption Site and Energy. The adsorption of PMDA–ODA fragment on several surface sites on the (100) metal surface was considered to get an overall picture of energies and relaxed geometry. The schematic drawing and the side view of the optimized model are shown in Figure 1 which also indicates the atoms and rings. Beginning with a relaxed PMDA–ODA structure that has been optimized separately, we find that the surface-adsorbed PMDA–ODA fragment deviates from its starting planar configuration; the two phenol rings twist out of the plane after optimization. The length of the monomer unit from oxygen atom to oxygen atom is 17.98 Å, which is consistent with previous theoretical and experimental data.¹⁴

To investigate the adhesion behavior between the PMDA–ODA fragment and the M(100) surface, four high-symmetry adsorption sites were considered. These adsorption positions were selected relative to the central aromatic ring (RII) in the PMDA part. Figure 2 indicates the four starting configurations, which include adsorption on the top site, the bridge A site (atoms C1 and C2 on the top sites), the bridge B-1 site (atoms C1 and C2 on the hollow sites), and bridge B-2 site (atoms C1 and C2 on the hollow sites and the PMDA–ODA is reversed leading to O9 and O10 at two ends closing to top M atoms), always with respect to the center of the RII ring. In this work, the adsorption energy is defined as $E_a = E_{\text{tot}} - E_{\text{clean}} - E_p$, where E_{tot} is the total energy of the slab with PMDA–ODA fragment, E_{clean} is the energy of the clean metal surface, and E_p is the energy of the isolated PMDA–ODA fragment.²⁷ By definition, $E_a < 0$ corresponds to exothermic chemical bonding. For Cu(100) (Table 1), the most favorable adsorption site is the bridge B-2, with an E_a

(17) Wu, P.; Jin, H. M.; Liu, H. L. *J. Adhes. Sci. Technol.* **2003**, *17*, 1075–1081.

(18) Wu, P.; Jin, H. M.; Liu, H. L. *J. Mater. Sci.* **2003**, *38*, 1727–1729.

(19) Mittendorfer, F.; Hafner, J. *Surf. Sci.* **2001**, *472*, 133–153.

(20) Kresse, G.; Hafner, J. *Phys. Rev. B* **1993**, *48*, 13115–13118.

(21) Kresse, G.; Hafner, J. *Phys. Rev. B* **1994**, *49*, 14251–14269.

(22) Blochl, P. E. *Phys. Rev. B* **1994**, *50*, 17953–17979.

(23) Kresse, G.; Joubert, D. *Phys. Rev. B* **1999**, *59*, 1758–1775.

(24) Perdew, J. P.; Wang, Y. *Phys. Rev. B* **1992**, *45*, 13244–13249.

(25) Wyckoff, R. W. G. *Crystal structures*, 2nd ed.; Interscience: New York, 1963.

(26) *CRC Handbook of Chemistry and Physics*, 79th ed.; CRC Press: Boca Raton, FL, 1998.

(27) Puisto, A.; Pitkanen, H.; Alatalo, M.; Jaatinen, S.; Salo, P.; Foster, A. S.; Kangas, T.; Laasonen, K. *Catal. Today* **2005**, *100*, 403–406.

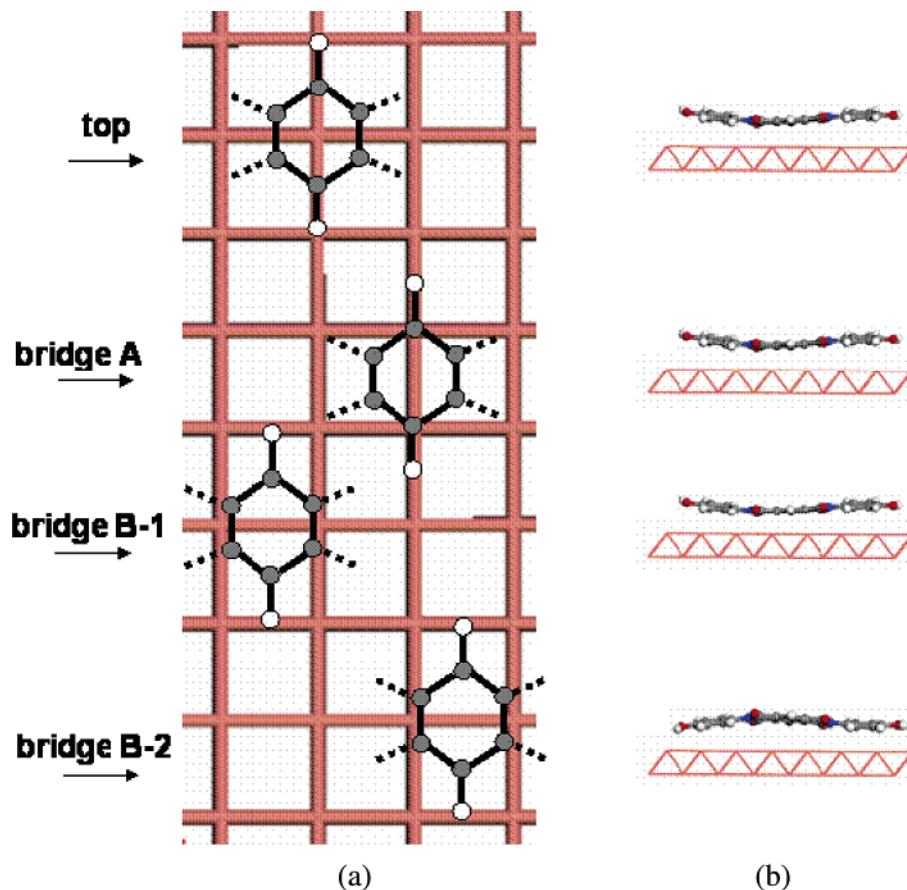


Figure 2. (a) Starting positions for polyimide adsorbed on M(100) surface with respect to the center benzene ring (RII) in the PMDA part; (b) side view of the PI/M(100) system at starting positions.

Table 1. Adsorption Energies for PI at Different Adsorption Sites on M(100) Surface

initial position	E_a (eV)	
	Cu(100)	Ni(100)
Top	-0.57	-4.71
Bridge A	-0.06	-3.68
Bridge B-1	-0.50	-1.72
Bridge B-2	-0.58	-4.68

of -0.58 eV, followed by the top site with the very similar value of -0.57 eV, and then bridge B-1, -0.50 eV, and bridge A, -0.06 eV. We note that the top site and bridge B-2 site on Cu(100) have very similar adsorption energies; thus, PI will competitively adsorb at these two sites on the Cu surface.

The top site is not stable for the PMDA-ODA/Ni(100) system anymore. After full optimization the RII ring in PMDA-ODA shifts to the bridge A site from its starting top site. Thus, we rename the top site on the Ni(100) surface as “bridge A-t”. For Ni(100) adsorption, we have bridge A-t (-4.71 eV) > bridge B-2 (-4.68 eV) > bridge A (-3.68 eV) > bridge B-1 (-1.72 eV) in decreasing order of adsorption energies. Obviously, the two bridge sites are competitive adsorption sites for PMDA-ODA/Ni(100) adsorption systems. A comparison of the two M(100) systems shows that PMDA-ODA adheres better to the Ni(100) surface than to the Cu(100) one.

3.2. Adsorption Geometry. The important optimized geometry parameters of PMDA-ODA adsorbed on M(100) surfaces are summarized in Table 2, while optimized

structures of PMDA-ODA adsorbed at “bridge B-2” on Cu(100) and PMDA-ODA adsorbed at “bridge A-t” on Ni(100) are shown in Figure 3. The geometry of PMDA-ODA is very different on the copper and nickel surfaces. On Cu(100), the RII ring tilts with the carbonyl oxygens closest to the surface and the phenol ODA portion parallel to the metal surface, whereas on the Ni(100) surface, the entire polymer unit is parallel to the metal surface with very little tilting of the rings.

Apart from bridge A sites, all adsorbed PMDA-ODA fragments on other sites on Cu(100) have the PMDA moiety as well as the two terminal benzene rings tilted along the y direction, with specific tilted angles compared to the copper surface. In the case of the bridge A site, the PMDA maintains a parallel configuration to the copper surface after relaxation; consequently, the difference in adsorption style leads to a deviation of adsorption energy. It is interesting to note that the most stable bridge B-2 site has the largest tilts angles (see Table 2). This result is consistent with Chen et al.’s studies on benzene adsorption on Cu(100).²⁸ They showed

(28) Chen, W.-K.; Cao, M.-J.; Liu, S.-H.; Xu, Y.; Li, J.-Q. *Chem. Phys. Lett.* **2005**, *407*, 414–418.

(29) Okamoto, Y. *Chem. Phys. Lett.* **2005**, *405*, 79–83.

(30) Xu, Y.; Mavrikakis, M. *Surf. Sci.* **2001**, *494*, 131–144.

(31) Shustorovich, E.; Bell, A. T. *Surf. Sci.* **1992**, *268*, 397–405.

(32) Torras, J.; Lacaze-Dufaure, C.; Russo, N.; Ricart, J. M. *J. Mol. Catal. A* **2001**, *167*, 109–113.

(33) Yamagishi, S.; Jenkins, S. J.; King, D. A. *Surf. Sci.* **2003**, *543*, 12–18.

(34) Mittendorfer, F.; Eichler, A.; Hafner, J. *Surf. Sci.* **1999**, *433–435*, 756–760.

Table 2. Various Optimized Geometry Parameters for PI at Different Adsorption Sites on M(100) Surface^a

	d_{C-M} (Å)	d_{RI} (Å)	d_{RII} (Å)	d_{RIII} (Å)	α (deg)	β (deg)	γ (deg)
Cu(100)							
top		3.07	3.21	3.22	3.54	-16.12	9.26
bridge A	2.200	3.18	2.42	2.88			
bridge B-1		3.38	3.13	3.31	11.56	-21.53	5.86
bridge B-2		3.25	3.40	3.23	8.53	-24.94	6.62
Ni (100)							
top	1.962–2.273	1.95	1.86	1.90			
bridge A	1.973–2.254	2.02	1.96	1.98			
bridge B-1	2.043–2.143	2.73	1.96	3.10			
bridge B-2	2.021–2.225	1.90	2.69	1.95			

^a α is the tilted angle between the RI and M plane. β is the tilted angle between the RII and M plane. γ is the tilted angle between the RIII and M plane. d_{RI} , d_{RII} , and d_{RIII} are the average distance from RI, RII, and RIII to the metal surface, respectively.

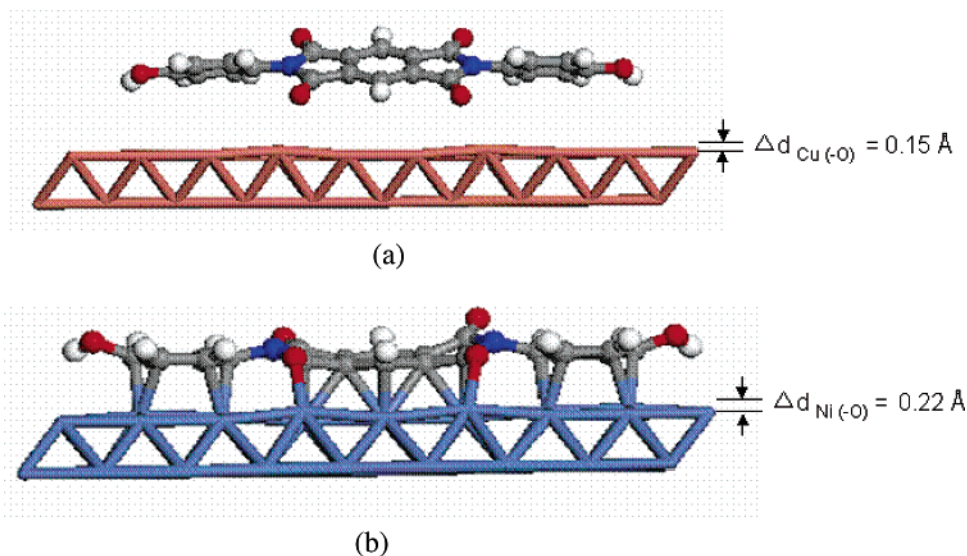


Figure 3. Optimized structures of PI adsorbed on a M(100) surface: (a) PI adsorbed on Cu(100) at bridge B-2 site; (b) PI adsorbed on Ni(100) at “bridge A-t”. $\Delta d_{M(-O)}$ is the upward shift of surface metal atom interacting with O atom in C=O.

Table 3. Important Parameters and Charge Transfer for Two Most Stable PI/M(100) System

	$d_{C3=O5, C4=O6(-M)}$ (Å)	$d_{O5-M, O6-M}$ (Å)	Δe^*			
			O5/O6	N7/N8	total C	PI–M
Cu–bridge B-2	1.257, 1.255	2.245, 2.257	-0.02	-0.01	-0.092	-0.15
Ni–“bridge A-t”	1.301, 1.301	2.001, 2.002	-0.05	-0.02/-0.05	-1.21	-1.60

^a Total charge change on O5, O6, N7, N8, all C atoms, and PI fragment, respectively. Negative value means charge transfer from adsorbate to metal substrate.

that the benzene molecule is tilted at high coverage. With combination of our results and theirs, the conclusion can be drawn that a tilt of the benzene ring is favorable for the adsorption of PMDA–ODA on the Cu(100) surface.

Again, the Ni(100) surface is quite different. As shown in Figure 3b, the PMDA–ODA monomer at “bridge A-t” forms many C–Ni interactions and is almost parallel to the Ni surface. Consequently, the interaction between the Ni surface and the PI is much stronger. Comparing the four adsorption sites, we notice that d_{RI} (2.73 Å) and d_{RIII} (3.10 Å) at the most unstable bridge B-1 site are noticeably longer than those at other adsorption sites (~ 1.95 Å) due to the two benzene rings tilting with respect to the Ni surface. Hence, for the nickel surface, parallel adsorption of a PMDA–ODA fragment is preferred.

3.3. Effect of Functional Groups in Polyimide. As we know, polyimide contains many functional groups, such as phenyl rings in the ODA part and carbonyl groups (C=O)

and C–N functions in the PMDA part. Thus, besides understanding the general conformation of PI on the metal, understanding the individual contributions of the various functional groups is also very important. Here we focus only on the most favorable positions adsorption sites for the metals, namely, bridge B-2 for copper and “bridge A-t” for nickel. Table 3 lists relevant bond lengths and charge transfer information. We notice that, for the isolated PMDA–ODA monomer, the C=O bond length is 1.221 Å, while when the PI is placed on the metal, the bond length stretches to 1.26 Å for copper and 1.30 Å for nickel. This shows that this bond is weakened when it is on the metal and that the bond is weaker for nickel than it is for copper. Alternatively, a weak bond is formed between the carbonyl oxygen and the metal.

Along with this bond formation, there is a distortion of the metal surface. In the copper, there is a deformation of about 0.15 Å and the nickel surface is pulled toward the

Table 4. Adsorption Energies for O/O₂ Adsorbed on Cu/Ni Surface in Previous Theoretical Studies

surface	O	O ₂
Cu(111)	-1.81, ^a -4.29, ^b -4.47 ^c (exp)	-0.67, ^a -0.56 ^b
Cu(100)	-2.42 ^d	-1.33 ^e
Ni(111)	-2.32 ^f	-1.67 ^g

^a Reference 29. ^b Reference 30. ^c Reference 31. ^d Reference 27. ^e Reference 32. ^f Reference 33. ^g Reference 34.

carbonyl of PI by 0.22 Å as shown in Figure 3. The metal–carbon bonds that are created are 2.25 Å for copper and 2.00 Å for nickel. There is probably a balance of this interaction and the interaction of the phenyl rings, which prefer the hollow site of the metal surface.¹⁹

In addition, there is a charge transfer from the polymer to the metal. Our calculation of total charge indicates that 1.60 electrons are transferred from the PI to the nickel, in agreement with Ramos's result¹⁴ (Table 3), but only 0.15 electrons are transferred to the copper. Clearly, this is the result of the better adhesion for the nickel system and indicates that there is little meaningful copper–polymer bonding. For nickel, most of the charge is transferred from the carbon (1.21 electrons). This indicates that there is a strong interaction between all parts of the PMDA–ODA and the nickel surface. The difference in charge is very small for the carbonyl oxygen (0.05 electrons) on nickel but even smaller on copper (0.02 electrons). This implies some weak bonding between the C–O–M. This result is consistent with XPS studies on a Cu/polymer interface.^{11,13} Since the carbonyl–copper bond is the most important interaction between the PI and copper surface on a per atom basis, it controls the charge-transfer properties at the PI/Cu interface. For example, O₂ plasma-treated polymer film has better adhesion with Cu than that subjected to N₂ and H₂/He mixture plasma treatment.⁸

3.4. Stability of Metal–Polyimide Composite. The weak interaction between unique reactive group C=O and Cu leads to poor adhesion in the PI/Cu(100) system. This motivates us to further consider the stability of metal filler in metal/polyimide composite in the air. Recently, many DFT calculations have investigated the adsorption of O atom and O₂ molecule on the Cu and Ni surface. Some theoretical and experimental results are listed in Table 4. We find that O/O₂ is more energetically favorable on the Cu(100) surface than

PMDA–ODA fragment. This result suggests that Cu–polyimide composite should be unstable in air conditions as amounts of oxygen will interact with copper and even replace existing polyimide; as a result, metal Cu particles will be oxidized. Obviously, the oxidation of copper filler in Cu–PI composite is mainly caused by oxygen from the ambient atmosphere. The finding is consistent with experimental observation. When the Cu/PI composite was kept in a nitrogen atmosphere, no oxidation was observed. When the Cu/PI was put in air, oxidation of Cu particles occurred in a week.

For the polyimide–Ni interface, due to interaction between multiple functional groups and Ni surface and perhaps some lattice matching, adhesion of the Ni(100)/PMDA–ODA system (E_a up to 4.71 eV) is much stronger than not only the corresponding Cu(100) adsorption system but also the oxygen/Ni adsorption system. The good adhesion with PI makes Ni a prospective candidate for metal–polymer composite with high dielectric constant.

4. Conclusions

In this work, we studied the interfacial properties of a PI/M(100) (M = Cu, Ni) system using ab initio calculations. We investigated four different adsorption sites on these metal surfaces and find that the “top site” is unstable for the Ni(100) surface. Polyimide fragment adopts “tilted” adsorption style on Cu(100) and “parallel” style on Ni(100) surface, which directly affects interfacial adhesion. Charge transfer can be observed from PI to metal substrate. The carbonyl functional group (C=O) in the PI can participate in weak M–O–C interaction. The Ni(100) surface displays better adhesion with polyimide than Cu(100) as more functional groups in the PI interact with the nickel surface. Good adhesion at PI/Ni(100) suggests that nickel is a better candidate as a metal filler than Cu in a metal–polyimide composite.

Acknowledgment. The authors are thankful for financial support from the Agency for Science, Technology and Research (A*STAR) of Singapore for the Singapore–China joint research project and for discussions with our partners in China, Professors Zhu Baoku and Xu Zhikang.

CM052865N